PAPER

Check for updates

Thermodynamics of the Eu(III)–Mg–SO₄–H₂O and Eu(III)–Na–SO₄–H₂O systems. Part II: spectroscopy experiments, complexation and Pitzer/SIT models†

P. F. dos Santos, [ID] *[a] X. Gaona, [ID] *[a] A. Lassin, [ID] [b] A. Skerencak-Frech,[a] D. Fellhauer,[a] M. Altmaier[a] and B. Madé[c]

A time-resolved laser fluorescence spectroscopy (TRLFS) study was carried out to investigate the Eu(III)–SO₄ complexation at room temperature over a wide range of Na₂SO₄ concentrations (0–2 mol kg⁻¹). Spectroscopic observations confirm the step-wise formation of the aqueous complexes $Eu(SO_4)^+$, $Eu(SO_4)_2^-$ and $Eu(SO_4)_3^{3-}$ over the investigated Na₂SO₄ concentrations. Combining TRLFS data obtained in this study and solubility data reported in Part I of this work for the Eu₂(SO₄)₃–Na₂SO₄–H₂O and Eu₂(SO₄)₃–MgSO₄–H₂O systems, thermodynamic and activity models were derived based on the SIT and Pitzer formalisms. A combination of the geochemical calculation codes PhreeqC (SIT), PhreeSCALE (Pitzer) and the parameter estimation code PEST was used to determine the solubility products $\left(K_{s,0}^{\circ}\right)$ of Eu₂(SO₄)₃·8H₂O(cr) and Na₂Eu₂(SO₄)₄·2H₂O(cr), stability constants of the Eu(III)–SO₄ complexes (β_i^0), and the specific binary and ternary interaction parameters $(\varepsilon_{ij}, \beta_{ij}^{(0)}, \beta_{ij}^{(1)}, C_{ij}^{\phi}, \theta_{ik}, \Psi_{ijk})$ for both activity models. The thermodynamic constants determined in this work are discussed with reference to values available in the literature.

1. Introduction

The sulfate ion behaves as a ligand of moderate strength in the presence of hard Lewis acids such as lanthanides, Ln(III), and actinides, An(III).[1] The aqueous complexes resulting from these interactions have been extensively studied in the case of Ln(III), Am(III) and Cm(III).[2–10] The systems Eu(III)–Mg–SO₄–H₂O and Eu(III)–Na–SO₄–H₂O were approached in Part I of this work[11] with new solubility data and solid phase characterization using the Pitzer equations to derive the corresponding thermodynamic and activity models. As often considered with the Pitzer formalism, full dissociation was assumed and only binary and ternary Pitzer interaction parameters for Eu³⁺ with SO₄²⁻, Na⁺ and Mg²⁺ were accounted for, *i.e.*, the explicit formation of Eu(III) complexes with sulfate was disregarded. This approach accurately describes the solubility of Eu(III) in acidic, dilute to concentrated Na₂SO₄ and MgSO₄ aqueous systems, but ignores the ample spectroscopic evidence on the formation of complexes between Eu³⁺ and SO₄²⁻, *i.e.*, $Eu(SO_4)^+$, $Eu(SO_4)_2^-$ and $Eu(SO_4)_3^{3-}$. Such complexes with Ln(III) and An(III) are considered in most thermodynamic databases developed in the context of radioactive waste disposal applications, *e.g.*, NEA-TDB,[2] ThermoChimie,[12] PSI-Nagra[13] or THEREDA,[14] using either SIT or Pitzer models for activity corrections. However, these databases do not consider the double-salt identified in Part I of this work (Na₂Eu₂(SO₄)₄·2H₂O(cr)) and have the focus on lower sulfate concentrations (<0.1 M), thus neglecting the formation of $Eu(SO_4)_3^{3-}$ and disregarding ion interaction coefficients with SO₄²⁻.

The most relevant complexation studies dealing with the system Eu(III)–SO₄ are briefly summarized in the following. Equilibrium constants for aqueous complex formation in the reference state $(\log_{10} \beta_i^0)$ reported in these studies are listed in Table 1 and are used in the discussion of the results obtained in this work. Barnes[15] studied the complexation of Eu(III) with sulfate by spectrophotometry at 25 °C. The concentration of Eu(III) was 5.01 × 10⁻³ mol kg⁻¹, with Na₂SO₄ concentration ranging from 3.00 × 10⁻³ to 1.213 × 10⁻² mol kg⁻¹. NaClO₄ was used to adjust the ionic strength to *ca.* 0.05 mol kg⁻¹. Within these boundary conditions, the author reported the presence of $Eu(SO_4)^+$ only. Izatt *et al.*[6] determined calorimetrically the values $\log_{10} K$, $\Delta°H$ and $\Delta°S$ for the complexation of Eu(III) with sulfate. Calorimetric titrations were performed at 25 °C with 0.02 mol kg⁻¹ Eu(III) perchlorate solutions and tetra-

ªInstitute for Nuclear Waste Disposal, Karlsruhe Institute of Technology, Karlsruhe, Germany. E-mail: pedro.santos@kit.edu, xavier.gaona@kit.edu
ᵇWater, Environment, Process Development and Analysis Division, BRGM, Orléans, France
ᶜResearch and Development Division, ANDRA, Châtenay-Malabry, France
†Electronic supplementary information (ESI) available. See DOI: https://doi.org/10.1039/d3dt04323a

Table 1 Solubility and complexation constants for the $Eu_2(SO_4)_3$–Na_2SO_4–H_2O and $Eu_2(SO_4)_3$–$MgSO_4$–H_2O systems, as reported in the literature or determined in this work

Solubility reactions $\left(\mathrm{Log}_{10}K^{\circ}_{s,0}\right)$

Reactions	$\left(\mathrm{Log}_{10}K^{\circ}_{s,0}\right)$	References
$Eu_2(SO_4)_3 \cdot 8H_2O(cr) \leftrightarrow 2Eu^{3+}(aq) + 3SO_4^{2-}(aq) + 8H_2O(l)$	-12.71 ± 0.10^{f}	This work/SIT
	-12.80 ± 0.10^{f}	This work/Pitzer
	$-11.911^{a,d}$	Das et al.[28]
	$-11.232 \pm 0.02^{c,d}$	F. dos Santos et al.[11]
	$-9.11 \pm 0.10^{b,d}$	Jordan et al.[17]
	-10.20 ± 0.70^{d}	ThermoChimie[12]
$Na_2Eu_2(SO_4)_4 \cdot 2H_2O(cr) \leftrightarrow 2Na^+(aq) + 2Eu^{3+}(aq) + 4SO_4^{2-}(aq) + 2H_2O(l)$	-19.23 ± 0.03^{c}	This work
	-17.518^{d}	Das et al.[28]
	$-17.056 \pm 0.03^{c,d}$	F. dos Santos et al.[11]

Complexation reactions $\left(\mathrm{Log}_{10}\beta^{\circ}_{i}\right)$

Reactions	$\mathrm{Log}_{10}\beta^{\circ}_{i}$	References
$Eu^{3+} + SO_4^{2-} \leftrightarrow Eu(SO_4)^+$	3.41 ± 0.12^{c}	This work
	3.50 ± 0.30	ThermoChimie[12]
	3.35 ± 0.02	Barnes[15]
	3.54 ± 0.02	Izatt et al.[6]
	3.78 ± 0.10	Vercouter et al.[8]
	3.87 ± 0.13^{e}	McDowell and Coleman[16]
$Eu^{3+} + 2SO_4^{2-} \leftrightarrow Eu(SO_4)_2^-$	5.84 ± 0.15^{c}	This work
	5.77 ± 0.02	Jordan et al.[17]
	5.20 ± 0.30	ThermoChimie[12]
	5.38 ± 0.30	Vercouter et al.[8]
	5.32 ± 0.12	Izatt et al.[6]
	5.74^{e}	McDowell and Coleman[16]
$Eu^{3+} + 3SO_4^{2-} \leftrightarrow Eu(SO_4)_3^{3-}$	5.15 ± 0.12^{c}	This work
	5.09^{e}	McDowell and Coleman[16]
$Mg^{2+} + SO_4^{2-} \leftrightarrow Mg(SO_4)(aq)$	2.39 ± 0.03^{c}	This work/SIT
	2.23 ± 0.03	ThermoChimie[12]
$Na^+ + SO_4^{2-} \leftrightarrow NaSO_4^-$	0.94 ± 0.20	ThermoChimie[12]

[a] Value calculated from the Gibbs energies of formation proposed by the author together with the Gibbs energies of formation of each species from the ThermoChime database.[12] [b] Calculated from the Rard[29] solubility data and using the Davies equation[30] for ionic strength corrections. [c] Uncertainty = 2σ. [d] Calculated without considering aqueous complexation. [e] As recalculated by Jordan et al.[17] [f] Uncertainty increased as compared to the value of 2σ, i.e., ±0.03.

methylammonium sulfate. Thermometric titration curves were best described considering the formation of both $Eu(SO_4)^+$ and $Eu(SO_4)_2^-$. McDowell and Coleman[16] investigated the complexation of trivalent transplutonium actinides (Am, Cm, Bk, Cf and Es) and europium with sulfate by means of solvent extraction (1-nonyldecylamine sulfate in benzene) at $T = 25$ °C. Stability constants of the An(III)/Eu(III)–sulfate complexes were determined in H_2SO_4/Na_2SO_4 mixtures with 0.01 mol kg^{-1} ≤ $[SO_4]_{tot}$ ≤ 0.5 mol kg^{-1} and varying ionic strength. The authors reported the formation of the complexes An/Eu$(SO_4)^+$, An/Eu$(SO_4)_2^-$ and (for the first time) An/Eu$(SO_4)_3^{3-}$. Skerencak and co-workers[4] investigated the complexation of Cm(III) with sulfate by means of Time Resolved Laser Fluorescence Spectroscopy (TRLFS). Spectroscopic measurements were conducted at $T = 25$–200 °C, with 0.006 mol kg^{-1} ≤ $[SO_4]_{tot}$ ≤ 0.365 mol kg^{-1} and ionic strength adjusted to 1.0 mol kg^{-1} ≤ I_m ≤ 4.0 mol kg^{-1} with $NaClO_4$. The formation of the complexes $Cm(SO_4)^+$ and $Cm(SO_4)_2^-$ was observed at $T = 25$ °C, whereas the complex $Cm(SO_4)_3^{3-}$ only formed in aqueous solutions with $[Na_2SO_4]$ ≥ 0.1 M and T ≥ 100 °C. Vercouter et al.[8]

studied the complexation of Eu(III) with sulfate at $T = 23 \pm 1$ °C using TRLFS. Experiments were performed in $H_2SO_4/HClO_4$ and $Na_2SO_4/NaClO_4$ solutions with 10^{-4} mol kg^{-1} Eu(III). Within the investigated boundary conditions, the authors observed only the formation of the complexes $Eu(SO_4)^+$ and $Eu(SO_4)_2^-$, whereas the formation of $Eu(SO_4)_3^{3-}$ was considered negligible. In addition to the complexation constants for the (1,1) and (1,2) complexes, Vercouter et al.[8] reported also SIT ion interaction parameters (ε_{ij}) for the ionic pairs Eu^{3+}/SO_4^{2-}, $Eu(SO_4)^+/SO_4^{2-}$ and $Eu(SO_4)_2^-/Na^+$. We note that this is the only experimental study available to date that reports SIT parameters for these species. Recently, Jordan et al.[17] conducted a comprehensive critical review of the literature available for the Eu(III)–sulfate system. Following a similar approach as NEA-TDB, the authors provided selected thermodynamic values for the evaluated Eu(III) systems. Equilibrium constants selected by Jordan et al.[17] are also included in Table 1.

On the basis of the existing literature and considering the solubility data presented in Part I of this work,[11] a TRLFS study was conducted at room temperature over a wide range of

Na_2SO_4 concentrations (0–2 mol kg^{-1}). By combining the independent evidences obtained by TRLFS with our solubility data in the $Eu_2(SO_4)_3$–Na_2SO_4–H_2O and $Eu_2(SO_4)_3$–$MgSO_4$–H_2O systems,[11] thermodynamic properties and activity models (SIT and Pitzer) were derived accounting for the formation of Eu(III)–SO_4 aqueous complexes.

2. Experimental

2.1. Chemicals

Europium(III) sulfate octahydrate ($Eu_2(SO_4)_3 \cdot 8H_2O(cr)$, p.a., 99.9 wt%) and magnesium sulfate heptahydrate ($MgSO_4 \cdot 7H_2O$, p.a., 99.5 wt%) were obtained from ThermoFisher Scientific. Anhydrous sodium sulfate (Na_2SO_4, p.a., >99 wt%) was purchased from Merck. All solutions were prepared with ultrapure water purified with a Milli-Q academic apparatus (Merck Millipore, 18.2 M Ω cm, 22 ± 2 °C, pore size 0.22 μm).

2.2. TRLFS experiments

The Eu(III)–Na–SO_4–H_2O system was investigated with 26 independent samples containing 10^{-6} mol kg^{-1} Eu(III) and 0–2 mol kg^{-1} Na_2SO_4 (see ESI†). The pH was measured with combined pH–electrodes (type Orion Ross, Thermo Scientific) to confirm the weakly acidic conditions preventing Eu^{3+} hydrolysis and the formation of HSO_4^- (<1%) (see ESI†). The excitation laser beam was generated by a Nd:YAG (Surelite II Laser, Continuum) pumping a dye laser (Narrowscan Dye Laser, Radiant Dyes) as described in Skerencak et al.[4,5] The wavelength (λ_{ex}) was tuned to 394 nm, with a maximum laser energy of 2 mJ with a repetition rate of 10 Hz. Emission spectra were recorded over a range of 575–635 nm with a delay of 1 μs and a time window of 1 ms. The emission spectra of each sample were integrated into 1000 accumulations. The obtained spectra can be qualitatively interpreted by the position of the intensity of the $^5D_0 \rightarrow {}^7F_2$ transition peak (see also section 5.1.).

3. Thermodynamic modelling

Thermodynamic and (SIT, Pitzer) activity models derived in this work rely on the solubility experiments with $Eu_2(SO_4)_3 \cdot 8H_2O(cr)$ and $Na_2Eu_2(SO_4)_4 \cdot 2H_2O(cr)$ described in Part I of this study[11] in combination with new TRLFS data presented here. The formation of Eu(III)–SO_4 complexes is explicitly considered in the thermodynamic modelling, as evidenced by spectroscopic means. The following step-wise complexation reactions are expected to take place with increasing sulfate concentration in solution:

$$Eu^{3+} + iSO_4^{2-} \leftrightarrow Eu(SO_4)_i^{3-2i}; \ i = 1, 2, 3 \quad (1)$$
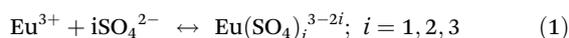
At the thermodynamic equilibrium, the stability constants in the reference state (β_i^0) can be expressed according to the law of mass action (2) – where a_i is the chemical activity of a given ion (unitless), with $a_j = \frac{m_j}{m_0} \cdot \gamma_j$. m_j and γ_j are the molality (mol kg^{-1}) and the activity coefficient (unitless) of the ion j,

respectively, at a given background electrolyte concentration and temperature, and $m_0 = 1$ mol kg^{-1} is the reference concentration. The term β_i refers to the conditional stability constant determined at a given ionic strength.

$$\beta_i^0 = \frac{a_{Eu(SO_4)_i^{3-2i}}}{(a_{Eu^{3+}})(a_{SO_4^{2-}}^i)} \quad (2)$$

$$\beta_i^0 = \frac{\left(m_{Eu(SO_4)_i^{3-2i}}\right)\left(\gamma_{Eu(SO_4)_i^{3-2i}}\right)}{(m_{Eu^{3+}})(\gamma_{Eu^{3+}})\left(m_{SO_4^{2-}}^i\right)\left(\gamma_{SO_4^{2-}}^i\right)} = \beta_i \frac{\left(\gamma_{Eu(SO_4)_i^{3-2i}}\right)}{(\gamma_{Eu^{3+}})\left(\gamma_{SO_4^{2-}}^i\right)} \quad (3)$$

In the present work, the activity coefficient (γ_i) is calculated using both the Pitzer equations as described in Part I of this study[11] and the Specific Ion Interaction Theory (SIT).[2,3,18] According to the SIT approach, the activity coefficient and the stability constant at infinite dilution (β_i^0) of an aqueous species i can be calculated according to:

$$\log_{10} \gamma_i = -z_i^2 D + \Delta_i(\varepsilon m)_{i,j} \quad (4)$$

$$\log_{10} \beta_i^0 = \log_{10} \beta_i - \Delta z^2 D + \Delta_i(\varepsilon m)_{i,j} \quad (5)$$

where m_j is the molal concentration of the species j other than i (mol kg^{-1}), $D = 0.509 I_m^{0.5}/(1 + 1.5 I_m^{0.5})$ is the Debye–Hückel term, z_i is the charge of the species i, Δz^2 is the stoichiometric difference of the squares of the charges of the products and reactants involved in the reaction, and $\varepsilon_{i,j}$ is the ion interaction coefficient between oppositely charged species i and j. For the chemical reactions described in (1), the equilibrium constants at infinite dilution and corresponding SIT-terms ($\Delta_n(\varepsilon m)$) can be calculated as follows:

$$\log_{10} \beta_1^0 = \log_{10} \beta_1 - 12D + \Delta_1(\varepsilon m) \quad (6)$$

For the Na_2SO_4 system :

$$\Delta_1(\varepsilon m) = \varepsilon_{Eu(SO_4)^+, SO_4^{2-}} m_{SO_4^{2-}} - \varepsilon_{Eu^{3+}, SO_4^{2-}} m_{SO_4^{2-}} - \varepsilon_{Na^+, SO_4^{2-}} m_{Na^+} \quad (7)$$

For the $MgSO_4$ system :

$$\Delta_1(\varepsilon m) = \varepsilon_{Eu(SO_4)^+, SO_4^{2-}} m_{SO_4^{2-}} - \varepsilon_{Eu^{3+}, SO_4^{2-}} m_{SO_4^{2-}} - \varepsilon_{Mg^{2+}, SO_4^{2-}} m_{Mg^{2+}} \quad (8)$$

$$\log_{10} \beta_2^0 = \log_{10} \beta_2 - 16D + \Delta_2(\varepsilon m) \quad (9)$$

For the Na_2SO_4 system :

$$\Delta_2(\varepsilon m) = \varepsilon_{Eu(SO_4)_2^-, Na^+} m_{Na^+} - \varepsilon_{Eu^{3+}, SO_4^{2-}} m_{SO_4^{2-}} - 2\varepsilon_{Na^+, SO_4^{2-}} m_{Na^+} \quad (10)$$

For the $MgSO_4$ system :

$$\Delta_2(\varepsilon m) = \varepsilon_{Eu(SO_4)_2^-, Mg^{2+}} m_{Mg^{2+}} - \varepsilon_{Eu^{3+}, SO_4^{2-}} m_{SO_4^{2-}} - 2\varepsilon_{Mg^{2+}, SO_4^{2-}} m_{Mg^{2+}} \quad (11)$$

$$\log_{10} \beta_3^0 = \log_{10} \beta_3 - 12D + \Delta_3(\varepsilon m) \quad (12)$$

For the Na_2SO_4 system :

$$\Delta_3(\varepsilon m) = \varepsilon_{Eu(SO_4)_3^{3-}, Na^+} m_{Na^+} - \varepsilon_{Eu^{3+}, SO_4^{2-}} m_{SO_4^{2-}} - 3\varepsilon_{Na^+, SO_4^{2-}} m_{Na^+} \quad (13)$$

For the MgSO$_4$ system :

$$\Delta_3(\varepsilon m) = \varepsilon_{\text{Eu}(\text{SO}_4)_3{}^{3-},\text{Mg}^{2+}} m_{\text{Mg}^{2+}} - \varepsilon_{\text{Eu}^{3+},\text{SO}_4{}^{2-}} m_{\text{SO}_4{}^{2-}} - 3\varepsilon_{\text{Mg}^{2+},\text{SO}_4{}^{2-}} m_{\text{Mg}^{2+}}$$

(14)

Chemical and thermodynamic models considered in this work include two solid phases, Eu$_2$(SO$_4$)$_3$·8H$_2$O(cr) and Na$_2$Eu$_2$(SO$_4$)$_4$·2H$_2$O(cr), and four europium aqueous species, Eu^{3+}, Eu(SO$_4$)$^+$, Eu(SO$_4$)$_2{}^-$ and Eu(SO$_4$)$_3{}^{3-}$, as well as the interaction parameters of the later ionic species with Na$^+$, Mg^{2+} and SO$_4{}^{2-}$ when oppositely charged. This allows a more realistic description of the aquatic chemistry of the investigated systems, at the cost of significantly increasing the number of parameters needed for accurate model calculations using Pitzer and SIT formalisms.

4. Parametrization procedure

The parameters required to reproduce the solubility and complexation of europium in the Eu$_2$(SO$_4$)$_3$–Na$_2$SO$_4$–H$_2$O and Eu$_2$(SO$_4$)$_3$–MgSO$_4$–H$_2$O systems are:

- Solubility products of the solid phases at I = 0, $\log_{10}K^\circ_{s,0}\{\text{Eu}_2(\text{SO}_4)_3 \cdot 8\text{H}_2\text{O}(\text{cr})\}$ and $\log_{10}K^\circ_{s,0}\{\text{Na}_2\text{Eu}_2(\text{SO}_4)_4 \cdot 2\text{H}_2\text{O}(\text{cr})\}$.

- Equilibrium constants of the Eu(III)–SO$_4$ aqueous complexes at I = 0, $\log_{10}\beta^0\{\text{Eu}(\text{SO}_4)^+\}$, $\log_{10}\beta^0\{\text{Eu}(\text{SO}_4)_2{}^-\}$ and $\log_{10}\beta^0\{\text{Eu}(\text{SO}_4)_3{}^{3-}\}$.

- Ion interaction parameters according to the SIT (ε_{ij}) and Pitzer ($\beta_{ij}^{(0)}$, $\beta_{ij}^{(1)}$, C_{ij}^ϕ, θ_{ik}) approaches.

The development of the Pitzer activity model for the investigated systems requires a total of 75 interaction parameters when considering all possible combinations of binary and ternary interactions. This includes 12 triplets of binary $\beta_{ij}^{(0)}$, $\beta_{ij}^{(1)}$, C_{ij}^ϕ, parameters (for two oppositely charged ions), 9 ternary θ_{ik} parameters (for two same-sign charged ions), and 30 ternary Ψ_{ijk} parameters (for cation/cation/anion or anion/anion/cation triplets). Most of them are neglected to avoid over-parameterization, in particular those involving interactions between two Eu(III) species and/or one ion of the background electrolyte. In the end, 18 parameters were considered most significant and thus included in the optimization process (see Table 2). Note that only 7 interaction parameters were required in Part I of this work to accurately describe the solubility datasets determined for the Eu$_2$(SO$_4$)$_3$–Na$_2$SO$_4$–H$_2$O and Eu$_2$(SO$_4$)$_3$–MgSO$_4$–H$_2$O systems, at the cost of disregarding Eu(III)–SO$_4$ aqueous complexes, i.e. assuming the only presence of Eu^{3+} in the aqueous phase.

The procedure of parameterization and development of the model is divided into three main stages:

(1) Verification of the databases used in the present work – ThermoChimie[12] and PhreeScale.[19] Using experimental osmotic coefficient data available in the literature[20–23] for the binary systems Na$_2$SO$_4$–H$_2$O and MgSO$_4$–H$_2$O, both databases are tested to verify the applicability limits within the salt con-

Table 2 SIT and Pitzer ion interaction coefficients determined in this work or reported in the literature for aqueous complexes in the Eu$_2$(SO$_4$)$_3$–Na$_2$SO$_4$–H$_2$O and Eu$_2$(SO$_4$)$_3$–MgSO$_4$–H$_2$O systems

SIT binary parameters

Species, i	Species, j	ε_{ij} (mol kg^{-1})	References	Species, i	Species, j	ε_{ij} (mol kg^{-1})	References
Eu^{3+}	SO$_4{}^{2-}$	0.86 ± 0.50	Vercouter et al.[8]	Mg^{2+}	Eu(SO$_4$)$_3{}^{3-}$	0.39 ± 0.30[a]	This work
Eu(SO$_4$)$^+$	SO$_4{}^{2-}$	−0.20 ± 0.12[a]	This work	Mg^{2+}	SO$_4{}^{2-}$	−0.27 ± 0.03[a]	This work
Na$^+$	Eu(SO$_4$)$_2{}^-$	−0.10 ± 0.04[a]	This work	Na$^+$	SO$_4{}^{2-}$	−0.12 ± 0.06	ThermoChimie[12]
Na$^+$	Eu(SO$_4$)$_3{}^{3-}$	−0.16 ± 0.04[a]	This work	Na$^+$	NaSO$_4{}^-$	0	This work
Mg^{2+}	Eu(SO$_4$)$_2{}^-$	0.48 ± 0.27[a]	This work	MgSO$_4$(aq)	Mg^{2+}, SO$_4{}^{2-}$	0	By definition in SIT

Pitzer parameters

Species, i	Species, j	$\beta_{ij}^{(0)}$	References	Species, i	Species, j	$\beta_{ij}^{(1)}$	References
Eu^{3+}	SO$_4{}^{2-}$	1.792	Fanghänel and Kim[9]	Eu^{3+}	SO$_4{}^{2-}$	15.040	Fanghänel and Kim[9]
Eu(SO$_4$)$^+$	SO$_4{}^{2-}$	−0.281	This work	Eu(SO$_4$)$^+$	SO$_4{}^{2-}$	1.560	NEA-TDB[3]
Na$^+$	Eu(SO$_4$)$_2{}^-$	−0.056	This work	Na$^+$	Eu(SO$_4$)$_2{}^-$	0.340	NEA-TDB[3]
Na$^+$	Eu(SO$_4$)$_3{}^{3-}$	0.137	This work	Na$^+$	Eu(SO$_4$)$_3{}^{3-}$	5.788	This work
Mg^{2+-}	Eu(SO$_4$)$_2{}^-$	0.990	This work	Mg^{2+}	Eu(SO$_4$)$_2{}^-$	1.843	This work
Mg^{2+}	Eu(SO$_4$)$_3{}^{3-}$	1.755	This work	Mg^{2+}	Eu(SO$_4$)$_3{}^{3-}$	8.744	This work

Species, i	Species, j	C_{ij}^ϕ	References	Species, i	Species, j	C_{ij}^ϕ	References
Eu^{3+}	SO$_4{}^{2-}$	0.600	Fanghänel and Kim[9]	Eu(SO$_4$)$^+$	SO$_4{}^{2-}$	0	This work
Na$^+$	Eu(SO$_4$)$_2{}^-$	0	This work	Mg^{2+}	Eu(SO$_4$)$_2{}^-$	0.921	This work
Na$^+$	Eu(SO$_4$)$_3{}^{3-}$	0	This work	Mg^{2+}	Eu(SO$_4$)$_3{}^{3-}$	−0.144	This work

Species, i	Species, k	θ_{ik}	References	Species, i	Species, k	θ_{ik}	References
Na$^+$	Eu(SO$_4$)$^+$	0	This work	Mg^{2+}	Eu(SO$_4$)$^+$	0.577	This work

[a] Uncertainty calculated as 2σ.

centrations considered in this study. If required, the available models are improved to extend their range of validity.

(2) Implementation of the SIT model. On the basis of the TRLFS results presented in this study and of solubility data reported in Part I of this work,[11] the parameters $\log_{10} K^{\circ}_{s,0}$, $\log_{10} \beta^0_i$ and ε_{ij} are simultaneously determined for the system $Eu_2(SO_4)_3–Na_2SO_4–H_2O$. Built on this model and in combination with solubility data reported for the $Eu_2(SO_4)_3–MgSO_4–H_2O$ system, ionic interaction parameters for the $MgSO_4$ system are derived.

(3) Implementation of the Pitzer model. The values of $\log_{10} K^{\circ}_{s,0}$ and $\log_{10} \beta^0_i$ obtained with the SIT model are adopted to ensure consistency among both activity models. On this basis, ion interaction parameters for the europium species are determined following a step-wise approach: (1) $Eu_2(SO_4)_3–Na_2SO_4–H_2O$ system considering both solubility and TRLFS data; (2) $Eu_2(SO_4)_3–MgSO_4–H_2O$ system based on solubility data.

The same approach as described in Part I of this work is considered for the optimization of the equilibrium constants and the ion interaction coefficients.[11] The PEST optimization software[24] is used in combination with the PhreeSCALE[19] (Pitzer formalism) or the Phreeqc3[25] (SIT model) codes and the databases described above. In addition to the calculation of the saturation ratio from solubility data, the independent normalized intensities of the TRLFS data (see section 5.1.) are used to fit the thermodynamic parameters of interest (solubility products, stability constants, ionic interaction parameters). The results of the calculations – solubility and normalized intensity – are compared to the corresponding experimental values by calculating the objective function that characterizes the deviation from the experimental data. In total, 45 solubility data and 26 TRLFS data with normalized intensity were used to derive SIT and Pitzer model parameters.

5. Results and discussion

5.1. TRLFS measurements

TRLFS spectra collected for Eu(III) (10^{-6} mol kg^{-1}) at increasing Na_2SO_4 concentrations (0–2 mol kg^{-1}) are shown in Fig. 1 (only $^7F_1$ and $^7F_2$ transition peaks shown). The spectra are normalized to equal total emission intesity for a better visualization of the change of the ratio of the $^7F_1$ to $^7F_2$ band with increasing ligand concentration. The $^7F_1$ (magnetic dipole) and $^7F_2$ (electric dipole) transition peaks are centered at 592 and 617 nm, respectively, and exhibit high sensitivity with increasing sulfate concentrations. The intensity of the $^5D_0 \rightarrow$ $^7F_2$ peak transition (so-called "hypersensitive transition") is significantly more influenced by the local symmetry of the Eu^{3+} ion and the nature of the ligands than by the intensities of the other electric dipole transitions.[8,26] A similar approach has been previously considered to evaluate the Eu(III)–SO_4 complexation in $NaClO_4–Na_2SO_4$ mixtures, although at lower total sulfate concentrations as those considered in the current study.[8]
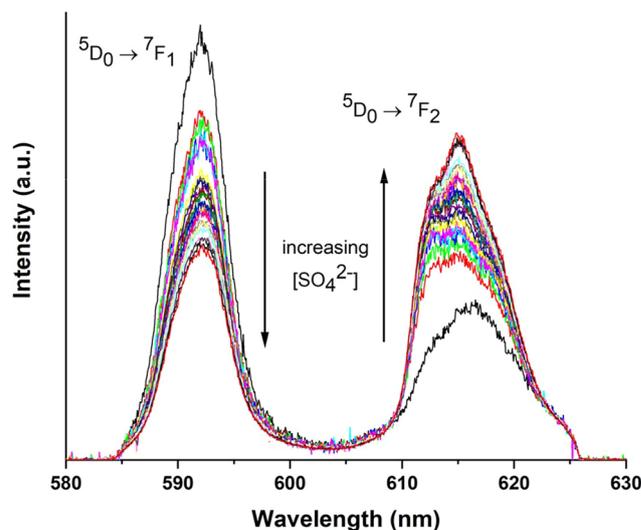

Fig. 1 TRLFS spectra of Eu(III) (10^{-6} mol kg^{-1}) with 0 mol kg^{-1} < [Na_2SO_4] < 2 mol kg^{-1}, in Na_2SO_4 aqueous solutions at room temperature. The spectra are normalized to equal emission intensity.

With increasing sulfate concentration in the system, the hypersensitive peak increases by more than 360%. The changes in the intensity of the $^5D_0 \rightarrow$ $^7F_2$ transition peak (at ~617 nm) are attributed to the formation of Eu(III)–sulfato complexes.[8,26] The quantitative analysis of the TRLFS spectra is thus based on these changes, as previously described by Vercouter et al.[8] The measured intensity (I_{mes}) is normalized (I^R_{norm}) with respect to the total concentration of Europium ([Eu(III)$_T$]), without a normalization to the total emission intensity, and the evolution of the Eu(III) fluorescence intensity is described according to:

$$I^R_{norm} = \frac{I_{mes}}{[\mathrm{Eu(III)}_T] I^o_0} = \frac{\sum\limits_{0 < i \leq 3} \left(I^R_i \beta_i [SO_4^{2-}]^i\right)}{\sum\limits_{0 < i \leq 3} \left(\beta_i [SO_4^{2-}]^i\right)} \quad (15)$$

With $I^R_i = I^o_i / I^o_0$, where I^o_i is the molar fluorescence intensity of the $Eu(SO_4)_i^{3-2i}$ species and I^o_0 is the molar fluorescence intensity in the absence of ligand (which means Eu^{3+} species). The β_i are the conditional stability constants defined in section 3. Therefore, in addition to the specific ion interaction coefficients (for the SIT and Pitzer models), the I^R_i intensities were also adjusted to obtain the complete model. Fig. 2 shows the experimental values of I^R_{norm} as a function of sulfate concentration, together with the calculations using the SIT and Pitzer models derived in this work. All experimental values are also provided in the ESI.†

5.2. Thermodynamic modelling

5.2.1. Binary systems $Na_2SO_4–H_2O$ and $MgSO_4–H_2O$.
As a first step in the process of deriving a complete set of equilibrium constants and ion interaction parameters for the ternary systems $Eu_2(SO_4)_3–Na_2SO_4–H_2O$ and $Eu_2(SO_4)_3–MgSO_4–H_2O$, the osmotic coefficient data available in the lit-

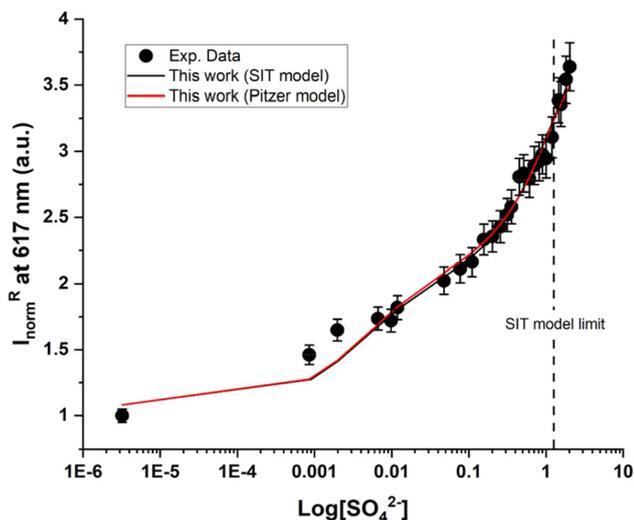**Fig. 2** Eu(III) normalized relative intensity (I_{norm}^{R}), at 617 nm as a function of Log[SO_4^{2-}], measured in Na_2SO_4 aqueous solutions containing 10^{-6} mol kg^{-1} Eu(III). Closed black circles: experimental data; full lines: models (black line: SIT, and red line: Pitzer). The vertical dashed line shows the validity limit of the SIT model as discussed in section 5.2.1.

erature for the binary systems Na_2SO_4–H_2O and $MgSO_4$–H_2O were used to re-evaluate model parameters. In the PhreeSCALE database, this verification was already done by Lach *et al.*[19,27] The PhreeSCALE database considers the full dissociation of the binary systems Na_2SO_4–H_2O and $MgSO_4$–H_2O. It is able to satisfactorily reproduce the experimental data of osmotic coefficient up to the saturation of the electrolytic solutions with respect to the $Na_2SO_4 \cdot 10H_2O$ (mirabilite) and $MgSO_4 \cdot 7H_2O$ (epsomite) solid phases, and beyond, as shown in Fig. 3a and b, respectively (red curves).

Fig. 3a shows that the ThermoChimie database (TDB) is able to correctly describe experimental osmotic coefficient data for the Na_2SO_4 system up to salt concentrations of ~1.45 mol kg^{-1}. Note that ThermoChimie considers the formation of the aqueous complex $NaSO_4^-$ with a $Log_{10}\beta_{1,1}^\circ = (0.936 \pm 0.20)$, but no value is provided for the SIT coefficient $\varepsilon_{NaSO_4^-, Na^+}$. The reevaluation of the $Log_{10}\beta_{1,1}^\circ$ and $\varepsilon_{NaSO_4^-, Na^+}$ parameters was attempted to improve the performance of the model. This exercise proved unsuccessful, and thus the $Log_{10}\beta_{1,1}^\circ$ value selected in ThermoChimie was retained, together with $\varepsilon_{NaSO_4^-, Na^+} = 0$.

ThermoChimie also includes the neutral complex $Mg(SO_4)(aq)$ with $Log_{10}\beta_{1,1}^\circ = (2.23 \pm 0.03)$. In contrast to the $NaSO_4$ system, Fig. 3b shows that this set of parameters only able to describe experimental values of the osmotic coefficients up to $MgSO_4$ concentrations of ~0.1 mol kg^{-1} (blue full line). To improve the performance of the available model, the values of $Log_{10}\beta_{1,1}^\circ$ and $\varepsilon_{SO_4^{2-}, Mg^{2+}}$ were fitted after the experimental osmotic coefficients. As a result, the revised values of $Log_{10}K_{s,0}^\circ$ and $\varepsilon_{SO_4^{2-}, Mg^{2+}}$ reported in Table 1 are able to accurately reproduce experimental data up to $MgSO_4$ concentration extended to 0.75 mol kg^{-1} (see Fig. 3b, black full line).
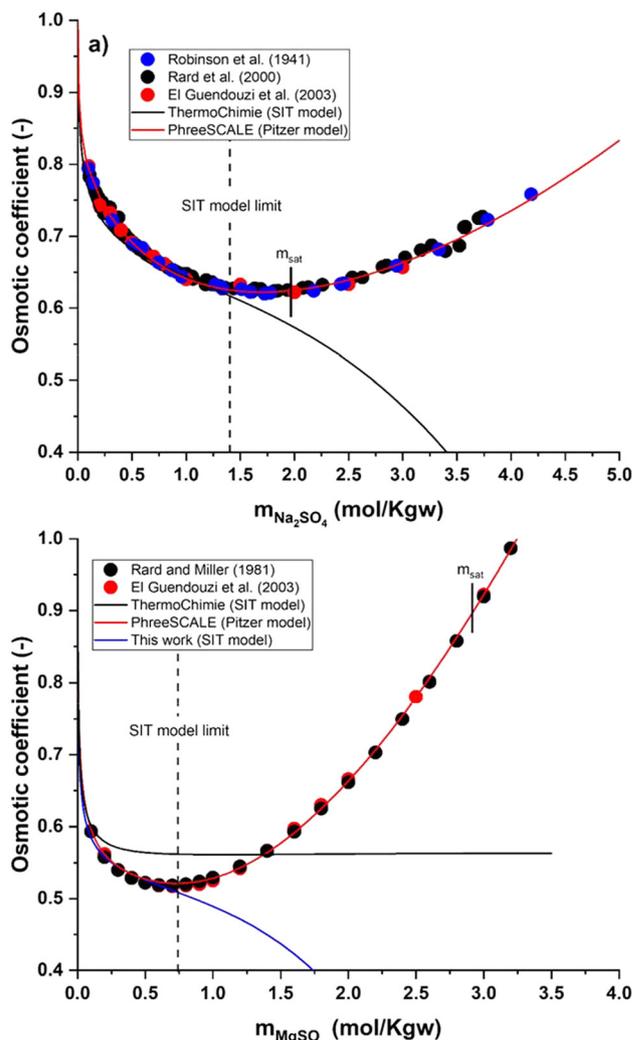

Fig. 3 (a) Osmotic coefficient of the Na_2SO_4–H_2O system at 25 °C as a function of Na_2SO_4 molality. (b) Osmotic coefficient of the $MgSO_4$–H_2O system at 25 °C as a function of $MgSO_4$ molality. Symbols are experimental or recommended values from the literature.[20–23] Lines are calculated values. Saturated solutions are indicated with the bars labelled m_{sat}.

5.2.2. Implementation of the SIT model

5.2.2.1. Ternary system $Eu_2(SO_4)_3$–Na_2SO_4–H_2O. The experimental data available for the $Eu_2(SO_4)_3$–Na_2SO_4–H_2O system – solubility and fluorescence intensities – were used to derive the values of $log_{10}K_{s,0}^\circ\{Eu_2(SO_4)_3 \cdot 8H_2O(cr)\}$, $log_{10}K_{s,0}^\circ\{Na_2Eu_2(SO_4)_4 \cdot 2H_2O(cr)\}$, $log_{10}\beta_1^\circ$, $log_{10}\beta_2^\circ$, $log_{10}\beta_3^\circ$, $\varepsilon_{Eu(SO_4)^+, SO_4^{2-}}$, $\varepsilon_{Eu(SO_4)_2^-, Na^+}$, $\varepsilon_{Eu(SO_4)_3^{3-}, Na^+}$, I_1^R, I_2^R and I_2^R. Vercouter *et al.*[8] proposed a value for the $\varepsilon_{SO_4^{2-}, Eu^{3+}}$ parameter, which we selected and therefore was not optimized in the present work. Jordan *et al.*[17] highlighted that the lack of experimental solubility data on the $Eu_2(SO_4)_3$–Na_2SO_4–H_2O system makes the evaluation of $\varepsilon_{SO_4^{2-}, Eu^{3+}}$ difficult, and suggested the use of isopiestic measurements for a more accurate determination of $\varepsilon_{SO_4^{2-}, Eu^{3+}}$. This is however not feasible due to the predominance of the Eu(III)–SO_4 complexes at $[SO_4^{2-}] >$

0.001 mol kg^{-1} and the relatively low solubility imposed by the sulfate salts of Eu(III). The fit of the available experimental data resulted in the thermodynamic parameters summarized in Tables 1 and 2, together with the values of $I_1^R = 1.081$, $I_2^R = 2.282$ and $I_3^R = 4.413$.

Experimental data and model calculations performed using the SIT model derived in this work are plotted (as black lines) in Fig. 2 for the normalized relative intensity and in Fig. 4 for the Eu(III) solubility in the Eu$_2$(SO$_4$)$_3$–Na$_2$SO$_4$–H$_2$O ternary system. Note that in spite of the limitations identified for the SIT model (m(Na$_2$SO$_4$) < 1.45 mol kg^{-1}, see section 5.2.1), the new set of parameters is able to reproduce satisfactorily all experimental observations. Additional details on the normalized intensity calculated with the SIT model ($I_{norm}^{R,SIT}$) are provided in the ESI.†

Table 2 summarizes the SIT ion interaction parameters $\varepsilon_{Eu(SO_4)^+, SO_4^{2-}}$, $\varepsilon_{Eu(SO_4)_2^-, Na^+}$ and $\varepsilon_{Eu(SO_4)_3^{3-}, Na^+}$ determined in this work. These values are consistent with those determined by Vercouter *et al.*[8] for the (1:1) and (1:2) complexes ($\varepsilon_{Eu(SO_4)^+, SO_4^{2-}} = -0.14 \pm 0.25$ mol kg^{-1} and $\varepsilon_{Eu(SO_4)_2^-, Na^+} = -0.05 \pm 0.07$ mol kg^{-1}), as well as those estimated by Hummel[18] for the (1,2) and (1,3) based on charge analogies ($\varepsilon_{Eu(SO_4)_2^-, Na^+} = -0.05 \pm 0.10$ mol kg^{-1}, $\varepsilon_{Eu(SO_4)_3^{3-}, Na^+} = -0.15 \pm 0.20$ mol kg^{-1}).

Fig. 5 shows the aqueous speciation Eu(III)-as a function of Na$_2$SO$_4$ concentration, calculated using the SIT model derived in this work (solid lines in the figure). As expected, europium is primarily found as complexed species (Eu(SO$_4$)$^+$) as soon as the Na$_2$SO$_4$ molality exceeds 0.0008 mol kg^{-1}. The complex Eu(SO$_4$)$_2^-$ dominates for ~0.07 < [Na$_2$SO$_4$] < ~1 mol kg^{-1}, whereas the (1,3) complex Eu(SO$_4$)$_3^{3-}$ becomes predominant only above the later concentration.

Fig. 4 Solubility in the system Eu$_2$(SO$_4$)$_3$–Na$_2$SO$_4$–H$_2$O at room temperature in logarithmic scale, according to SIT (black lines) and Pitzer (red lines) models. Symbols: experimental data reported in Part I of this work or in the literature.[11]
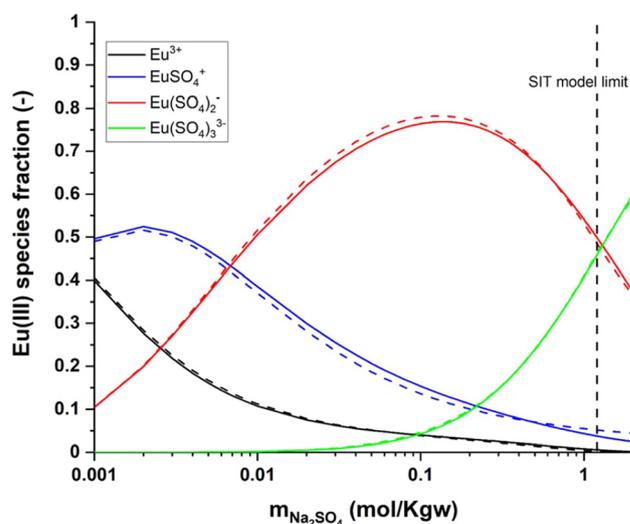

Fig. 5 Aqueous speciation of Eu(III) with increasing Na$_2$SO$_4$ concentrations at 25 °C, as calculated using the SIT (solid lines) and Pitzer (dashed lines) activity models derived in this work.

This study represents the most comprehensive work on the solubility and aqueous complexation of Eu(III) in sulfate media, providing a consistent set of solubility and complexation constants ($\log_{10} K_{s,0}^{\circ}\{Eu_2$(SO$_4$)$_3 \cdot$ 8H$_2$O(cr)$\}$, $\log_{10} K_{s,0}^{\circ}\{Na_2Eu_2$(SO$_4$)$_4 \cdot$ 2H$_2$O(cr)$\}$, $\log_{10} \beta_1^0$, $\log_{10} \beta_2^0$ and $\log_{10} \beta_3^0$) on the basis of new and previously reported experimental data. Table 1 shows that solubility constants derived in this work are in disagreement with $\log_{10} K_{s,0}^{\circ}\{Eu_2$(SO$_4$)$_3 \cdot$ 8H$_2$O(cr)$\}$ and $\log_{10} K_{s,0}^{\circ}\{Na_2Eu_2$(SO$_4$)$_4 \cdot$ 2H$_2$O(cr)$\}$ values reported in previous studies. This is explained by the fact that previous $\log_{10} K_{s,0}^{\circ}$ values were determined disregarding the formation of aqueous Eu(III)-sulfate complexes,[11,12,28] despite they form at very low sulfate concentration values like those resulting from the dissolution of Eu$_2$(SO$_4$)$_3$·8H$_2$O(cr) in water. The only value provided in the literature for $\log_{10} K_{s,0}^{\circ}\{Na_2Eu_2$(SO$_4$)$_4 \cdot$ 2H$_2$O(cr)$\}$ was estimated by Das *et al.*[28] The present work thus provides the first evidence for the experimental determination of this solubility product. The values of $\log_{10} \beta_1^0$ and $\log_{10} \beta_2^0$ determined in this work agree well with literature data when considering the corresponding uncertainties. Note that most of the previous studies were performed in the presence of mixed background electrolytes (NaClO$_4$–Na$_2$SO$_4$), with lower sulfate concentrations, and using the Debye–Hückel approach for ionic strength corrections in most cases.

The value of $\log_{10} \beta_3^0$ determined in this work based on solubility and spectroscopic data agrees within the corresponding uncertainties with the value determined by means of solvent extraction by McDowell and Coleman.[16] The original conditional equilibrium constant reported by the authors was recently extrapolated to $I = 0$ by Jordan *et al.*[17] using the Debye–Hückel equation. Note that ionic strength corrections with this method are less accurate at the high salt/acid concentrations considered in the original solvent extraction study.

5.2.2.2. Ternary system Eu₂(SO₄)₃–MgSO₄–H₂O. Solubility and complexation constants, as well as SIT coefficients for cationic species with SO_4^{2-} determined from solubility and spectroscopic data in the Na_2SO_4 system were kept constant for the modelling of the $MgSO_4$ system. Thus, only the parameters $\varepsilon_{Eu(SO_4)_2^-, Mg^{2+}}$ and $\varepsilon_{Eu(SO_4)_3^{3-}, Mg^{2+}}$ were fitted on the basis of Eu(III) solubility data reported in Part I of this work for $MgSO_4$ solutions (19 independent data points). The resulting parameters summarized in Table 2 are able to successfully reproduce the experimental solubility data (see black line in Fig. 6), in spite of the limitations identified in section 5.2.1 for the application of the SIT model to $MgSO_4$ solutions above 0.75 mol kg⁻¹. Fig. 7 shows the speciation diagram of Eu(III) calculated for the $Eu_2(SO_4)_3$–$MgSO_4$–H_2O system up to a $MgSO_4$ concentration of 2 mol kg⁻¹. As expected, the speciation diagram calculated for the $MgSO_4$ system presents close similarities with respect to the Eu(III) species distribution in Na_2SO_4 solutions (see Fig. 5). However, the calculated concentration of the $Eu(SO_4)^+$ complex unexpectedly increases above 1 M $MgSO_4$. This artifact of the model is partially attributed to the limited performance of the SIT model for the binary system $MgSO_4$–H_2O. Note that the formation of a ternary solid phase with Mg (analogous to $Na_2Eu(SO_4)_4 \cdot 2H_2O(cr)$ controlling the solubility in the Na_2SO_4 system) was not confirmed experimentally by XRD analysis. The formation of such a phase could be also responsible of the decrease in solubility observed above 1 M $MgSO_4$.

5.2.3. Implementation of the Pitzer model. The values of $\log_{10} K_{s,0}^{\circ}\{Eu_2(SO_4)_3 \cdot 8H_2O(cr)\}$, $\log_{10} K_{s,0}^{\circ}\{Na_2Eu(SO_4)_4 \cdot 2H_2O(cr)\}$, $\log_{10} \beta_1^0$, $\log_{10} \beta_2^0$, $\log_{10} \beta_3^0$, I_1^R, I_2^R and I_2^R were taken from the SIT model to maintain internal consistency between the models. To further minimize
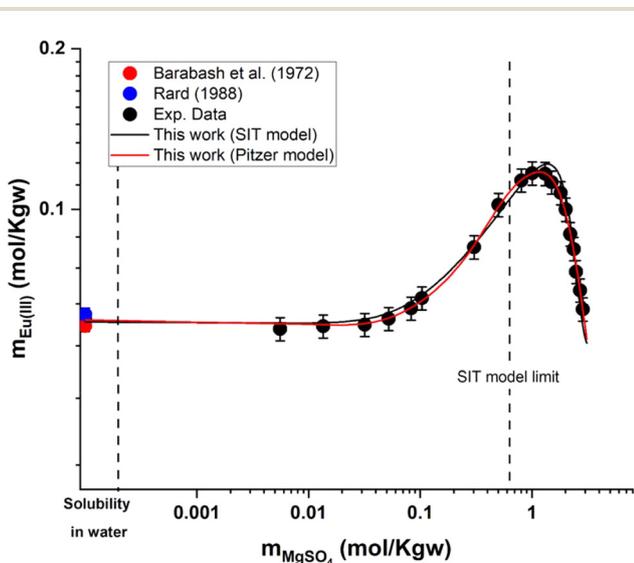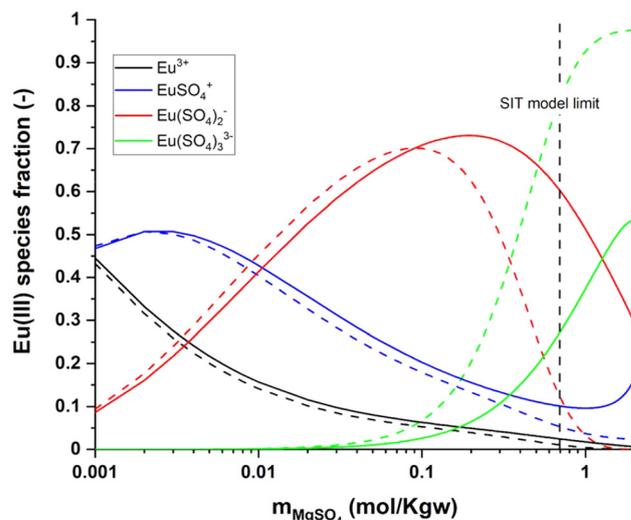

Fig. 7 Aqueous speciation of Eu(III) with increasing MgSO₄ concentrations at 25 °C, as calculated using the SIT (solid lines) and Pitzer (dashed lines) activity models derived in this work.

the number of fitting parameters and avoid over-parameterization, a number of Pitzer parameters were adopted from the literature. Fanghänel and Kim[9] determined $\beta_{Cm^{3+}, SO_4^{2-}}^{(0)}$, $\beta_{Cm^{3+}, SO_4^{2-}}^{(1)}$ and $C_{Cm^{3+}, SO_4^{2-}}^{\phi}$ based on Cm(III) TRLFS measurements. Considering the analogy between An(III) and Ln(III), Xiong et al.[31] adopted the same parameters for the description of the $Nd_2(SO_4)_3^{2-}$–H_2O system. These values have been also taken as fixed parameters, $\beta_{Eu^{3+}, SO_4^{2-}}^{(0)}$, $\beta_{Eu^{3+}, SO_4^{2-}}^{(1)}$ and $C_{Eu^{3+}, SO_4^{2-}}^{\phi}$, in the present work, in addition to the standard values of $\beta_{Eu(SO_4)_2^-, Na^+}^{(1)}$ and $\beta_{Eu(SO_4)^+, SO_4^{2-}}^{(1)}$ proposed in the NEA publication "Modelling in Aquatic Chemistry"[3] for (1 : 1) and (1 : 2) interactions.

Taking into account these assumptions and a slight modification in $\log_{10} K_{s,0}^{\circ}\{Eu_2(SO_4)_3 \cdot 8H_2O(cr)\}$ (from −12.71 to −12.80), we obtained binary Pitzer interaction parameters (see Table 2) that are able to satisfactorily reproduce both experimental solubility data and normalized intensity for the $Eu_2(SO_4)_3$–Na_2SO_4–H_2O system (red lines in Fig. 2 and 4). Moreover, Fig. 5 shows that this set of parameters results in a similar distribution of species as calculated with the SIT model. This underpins that both activity models provide a consistent description of the solubility and speciation in the $Eu_2(SO_4)_3$–Na_2SO_4–H_2O system.

In addition to $\beta_{Eu(SO_4)_2^-, Mg^{2+}}^{(0)}$, $\beta_{Eu(SO_4)_2^-, Mg^{2+}}^{(1)}$, $\beta_{Eu(SO_4)_3^{3-}, Mg^{2+}}^{(0)}$ and $\beta_{Eu(SO_4)_3^{3-}, Mg^{2+}}^{(1)}$, the incorporation of the parameters $C_{Eu(SO_4)_2^-, Mg^{2+}}^{\Phi}$, $C_{Eu(SO_4)_3^{3-}, Mg^{2+}}^{\Phi}$ and $\theta_{Eu(SO_4)^+, Mg^{2+}}$ was required to properly explain the solubility data in the $Eu_2(SO_4)_3$–$MgSO_4$–H_2O system (see Fig. 6, and Fig. SI-1 in the ESI†). The speciation diagram calculated with this model is shown in Fig. 7 (dashed lines corresponding to the Pitzer model). The figure underpins a good agreement between the SIT and Pitzer speciation calculations up to a sulfate molality of ∼0.1 mol kg⁻¹. Above this sulfate concentration, the Pitzer model predicts a greater stability of the complex $Eu(SO_4)_3^{3-}$ with increasing

Fig. 6 Solubility in the system Eu₂(SO₄)₃–MgSO₄–H₂O at room temperature in logarithmic scale, according to SIT (black line) and Pitzer (red line) models. Symbols: experimental data as reported in Part I of this work or in the literature.[11]

$MgSO_4$ concentration. Considering the limitations of SIT at high ionic strength conditions, and in particular those identified for the SIT model of the binary $MgSO_4–H_2O$ system (see section 5.2.1), a higher reliability is attributed to the Pitzer speciation model at high $MgSO_4$ concentrations. Based on solubility and TRLFS measurements, Herm *et al.*[10] proposed the formation of ternary complexes betwn Mg, Cm(III)/Nd(III) and nitrate at high $Mg(NO_3)_2$ concentrations. In line with these observations, the enhanced stability of the $Eu(SO_4)_3^{3-}$ complex predicted by the Pitzer model in the $MgSO_4$ compared to the Na_2SO_4 system could be attributed to the strong interaction expected between this anionic species with charge -3 and a divalent cation like Mg^{2+}. Attempting to include a ternary complex (*e.g.* $Mg[Eu(SO_4)_3]^-$) in the chemical model was unsuccessful, and this option was disregarded as the species is not required to properly explain solubility.

6. Summary and conclusions

The complexation of Eu(III) with sulfate in dilute to concentrated Na_2SO_4 solutions (0–2 mol kg^{-1}) was studied at room temperature by means of TRLFS. Sulfate has a significant influence on the hypersensitive emission peak $^5D_0 \rightarrow {}^7F_2$ of the Eu(III) spectra. The evaluation of TRLFS data collected for the $Eu_2(SO_4)_3–Na_2SO_4–H_2O$ system allows the identification of three main aqueous complexes, *i.e.*, $Eu(SO_4)^+$, $Eu(SO_4)_2^-$ and $Eu(SO_4)_3^{3-}$. The combination of these TRLFS results with solubility data determined in Part I of this work for the systems $Eu_2(SO_4)_3–Na_2SO_4–H_2O$ and $Eu_2(SO_4)_3–MgSO_4–H_2O$, allows deriving complete chemical, thermodynamic and activity models based on both the SIT and Pitzer formalisms.

Both activity models are able to successfully and consistently describe solubility and TRLFS data in the $Eu_2(SO_4)_3–Na_2SO_4–H_2O$ system. Equilibrium constants derived in this work for the complexes $Eu(SO_4)^+$, $Eu(SO_4)_2^-$ and $Eu(SO_4)_3^{3-}$ agree well with those previously reported in the literature. Discrepancies with $\log_{10} K_{s,0}^\circ \{Eu_2(SO_4)_3 \cdot 8H_2O(cr)\}$ in the literature are harmonized when considering the formation of Eu(III)–SO_4 complexes, which become predominant already at the sulfate concentrations defined by the solubility of this solid phase in water. The value of $\log_{10} K_{s,0}^\circ \{Na_2Eu_2(SO_4)_4 \cdot 2H_2O(cr)\}$ determined in this work is based on the first experimental evidence available to date.

SIT and Pitzer activity models derived in this work describe well the solubility data available for the $Eu_2(SO_4)_3–MgSO_4–H_2O$ system. However, both models provide discrepant speciation schemes at high $MgSO_4$ concentrations, which can be due to: (i) limitations of the thermodynamic data available for the binary system $MgSO_4–H_2O$, (ii) the possible formation of a ternary complex Mg–Eu(III)–SO_4 at high $MgSO_4$ concentrations, currently not included in the model, (iii) the possible formation of a ternary solid phase Mg–Eu(III)–SO_4 (analogous to the $Na_2Eu_2(SO_4)_4 \cdot 2H_2O(cr)$ observed in the Na_2SO_4 system) that would explain the decrease in solubility observed at high $MgSO_4$ concentrations, or (iv) a combination of (i)–(iii).

This work is the second of a series targeting the thermodynamic description of complex Ln(III)/An(III)–SO_4–NO_3 systems of relevance in the context of radioactive waste disposal.

Conflicts of interest

There are no conflicts to declare.

Acknowledgements

References

1 M. Altmaier, X. Gaona and T. Fanghänel, *Chem. Rev.*, 2013, **113**, 901–943.

2 NEA, *Second update on the Chemical Thermodynamics of Uranium, Neptunium, Plutonium, Americium And Technetium*, OECD, 2021, vol. 14.

3 NEA, *Modelling in Aquatic Chemistry*, OECD Publishing, Paris, 2020.

4 A. Skerencak, P. J. Panak and T. Fanghänel, *Dalton Trans.*, 2013, **42**, 542–549.

5 A. Skerencak, P. J. Panak, W. Hauser, V. Neck, R. Klenze, P. Lindqvist-Reis and T. Fanghänel, *Radiochim. Acta*, 2009, **97**(8), 385–393.

6 R. M. Izatt, D. Eatough, J. J. Christensen and C. H. Bartholomew, *J. Chem. Soc. A*, 1969, 47–53.

7 I. L. Jenkins and C. B. Monk, *J. Am. Chem. Soc.*, 1950, **72**, 2695–2698.

8 T. Vercouter, B. Amekraz, C. Moulin, E. Giffaut and P. Vitorge, *Inorg. Chem.*, 2005, **44**, 7570–7581.

9 T. Fanghänel and J.-I. Kim, *J. Alloys Compd.*, 1998, **271–273**, 728–737.

10 M. Herm, X. Gaona, T. Rabung, D. Fellhauer, C. Crepin, K. Dardenne, M. Altmaier and H. Geckeis, *Pure Appl. Chem.*, 2015, **87**, 487–502.

11 P. F. dos Santos, A. Lassin, X. Gaona, K. Garbev, M. Altmaier and B. Madé, *Dalton Trans.*, 2024, DOI: **10.1039/d3dt04322c**.

12 E. Giffaut, M. Grivé, P. Blanc, P. Vieillard, E. Colàs, H. Gailhanou, S. Gaboreau, N. Marty, B. Madé and L. Duro, *Appl. Geochem.*, 2014, **49**, 225–236.

13 W. Hummel and T. Thoenen, *The PSI Chemical Thermodynamic Database 2020*, 2023.

14 H. C. Moog, F. Bok, C. M. Marquardt and V. Brendler, *Appl. Geochem.*, 2015, **55**, 72–84.

15 J. C. Barnes, *J. Chem. Soc.*, 1964, 3880.

16 W. J. McDowell and C. F. Coleman, *J. Inorg. Nucl. Chem.*, 1972, **34**, 2837–2850.

17 N. Jordan, T. Thoenen, S. Starke, K. Spahiu and V. Brendler, *Coord. Chem. Rev.*, 2022, **473**, 214608.

18 W. Hummel, *Ionic strength corrections and estimation of SIT ion interaction coefficients*, Villigen, Switzerland, 2009.

19 A. Lach, F. Boulahya, L. André, A. Lassin, M. Azaroual, J.-P. Serin and P. Cézac, *Comput. Geosci.*, 2016, **92**, 58–69.

20 C. K. Chan, Z. Liang, J. Zheng, S. L. Clegg and P. Brimblecombe, *Aerosol Sci. Technol.*, 1997, **27**, 324–344.

21 R. A. Robinson, J. M. Wilson and R. H. Stokes, *J. Am. Chem. Soc.*, 1941, **63**, 1011–1013.

22 M. E. Guendouzi, A. Mounir and A. Dinane, *J. Chem. Thermodyn.*, 2003, **35**, 209–220.

23 J. A. Rard and D. G. Miller, *J. Chem. Eng. Data*, 1981, **26**, 33–38.

24 J. Doherty, *PEST: Model-Independent Parameter Estimation*, 5th edn, 2004.

25 C. A. J. Appelo, *Appl. Geochem.*, 2015, **55**, 62–71.

26 K. Binnemans, *Coord. Chem. Rev.*, 2015, **295**, 1–45.

27 A. Lach, L. André and A. Lassin, *Appl. Geochem.*, 2017, **78**, 311–320.

28 G. Das, M. M. Lencka, A. Eslamimanesh, P. Wang, A. Anderko, R. E. Riman and A. Navrotsky, *J. Chem. Thermodyn.*, 2019, **131**, 49–79.

29 J. A. Rard, *J. Solution Chem.*, 1988, **17**, 499–517.

30 C. W. Davies, *Ion association*, Butterworths, London, 1962.

31 Y. Xiong, G. Xu and Y. Wang, *J. Solution Chem.*, 2023, **52**, 447–466.